A study of mixed-mode composite delamination using enriched interface elements

I. Guiamatsia
irene.guiamatsia@sydney.edu.au
School of Civil Engineering, The University of Sydney
Sydney, Australia

J. K. Ankersen and L. Iannucci
Department of Aeronautics, Imperial College London
London, UK

ABSTRACT

This paper examines the performance of enriching the shape functions of interface finite elements in the prediction of mixed-mode delamination. Enriching second-order interface and solid elements with the analytical solution of a beam on elastic foundation problem yields the correct displacement field ahead of the crack tip. Despite the enrichment being fixed at elements nodes, resulting in non-traceability of the crack tip location, the strategy is shown to perform consistently well, increasing the minimum element size from the typical 0·5mm to 5mm, for a range of classical mixed-mode bending (MMB) specimens.

1.0 INTRODUCTION

Delamination is the most widely encountered mode of failure in composite laminates, either in isolation or in conjunction with other failure mechanisms. For a numerical model to accurately predict the response of the composite structure under complex loading, it is crucial that each dissipative mechanism is faithfully captured. To achieve an 'automatic' and smooth advance of the crack front without remeshing, interface elements were introduced by Schellekens and De Borst[1]. These are finite elements that are used to connect nodes on either side of the interface and are equipped with a cohesive constitutive response (Dugdale[2] and Barenblatt[3]) featuring an initial elastic regime up to a yield point (interface strength), followed by either a plastic or softening

Paper No. 3918. Manuscript received 25 October 2012, revised version received 27 February 2013, accepted 1 March 2013.

https://doi.org/10.1017/S0001924000008617 Published online by Cambridge University Press

regime where a quantity of energy equal to the material's fracture toughness is dissipated. This technique has been implemented with various types of elements (e.g. discrete springs[4], continuum interfaces[1]) and constitutive responses, e.g. Refs 5-7.

The issue *du jour*, with respect to modelling composite delamination in realistically-sized structures, is the high computational cost that results from the need to utilise very small interface finite elements to represent the interface. This generally means that equally small elements are indeed required for the entire model as nodes are shared between interface and ply. The typical guideline of a few elements within the fracture process zone (FPZ), about 1mm for composite laminates, translates into a maximum element size that is of the order of 0·125 to 0·5mm.

The dramatic effect of the element size on the accuracy of the prediction is illustrated in Fig. 1, where a sensitivity on the interface element size is performed for the double cantilever beam (DCB), a standard benchmark of mode I composite delamination.

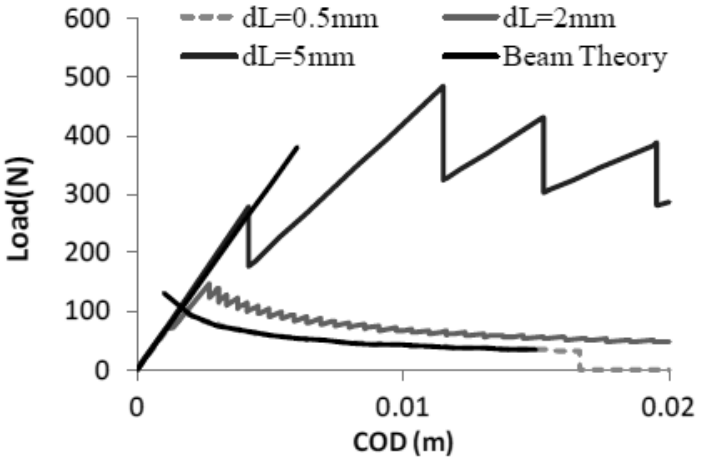


Figure 1. Mesh sensitivity for the DCB specimen.

An engineering solution was proposed by Turon *et al*[8] to enable the use of larger interface elements; this consisted of reducing the interface strength, which is roughly inversely proportional to the cohesive length if a bilinear interface constitutive response is assumed. However, while the energy dissipation is arguably the most important feature of a material damage model, correctly capturing the structural peak load can and will, in some cases, be influenced by the interface strength; hence the proposed adhoc reduction may, as shown in Fig. 2, yield some unexpected outcomes as seen for the mode II specimen. In this figure the analyses of the mode I (double cantilever beam) and mode II (end-notched flexure beam) were performed with a mesh size of 5mm. Similar inconsistencies have been reported elsewhere[10,14].

The idea of a partition of unity enrichment of interface element shape functions is relatively recent: Crisfield and Alfano[9] first enriched a linear interface element with cubic and quintic polynomials in order to successfully improve the smoothness of the predicted load in the propagation regime of a DCB, using a mesh size of 1mm. Samini *et al*[11,12] used an enrichment with hat functions so as to allow a bilinear separation within elements containing the crack tip, and applied their method to solve a mixed-mode peel off problem. Their focus was, as in Ref. 9, to improve the numerical performance of the solution by removing the non-physical oscillations that appear in the traction/

https://doi.org/10.1017/S0001924000008617 Published online by Cambridge University Press

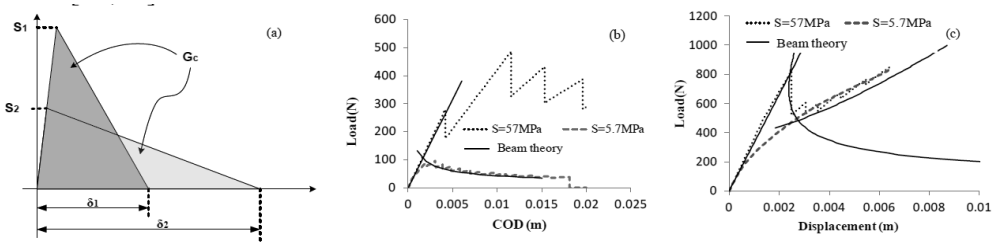


Figure 2. Effects of interface strength reduction (a) on cohesive zone length (b) on mode I response (c) on mode II response.

separation curve when coarse meshes were utilised. Note that what was termed a 'coarse' mesh was approximately 1·25mm, which is still fine enough for a non-enriched cohesive element (such as the one provided by the commercial package ABAQUS[19]) to correctly capture the peak load and post-peak behavior with a level of accuracy well within acceptable industry standards.

Van der Meer *et al*[13] recently proposed a different perspective based on a representation of the crack front using level set functions, with an initial element eventually split into two (upper and lower) elements, and fracture mechanics arguments used to quantify crack growth (crack front determined by the unbalance between energy release and fracture toughness, with energy release calculated via a VCCT-type approach). While the approach shows good results with good predictions of crack growth with 10mm mesh size, there are at least two reasons for which the approach is still far from practical readiness: (1) within a commercial finite element package, the implementation of the element splitting procedure (involving change in the model topology during the analysis) and of multiple level set fields (if there are many cracks, especially in 3D), is not straightforward, (2) In composites, delamination usually occurs between two layers of different orientations, and if several interfaces through the thickness fail simultaneously with different crack fronts, the proposed substitution of one-to-three elements quickly becomes cumbersome and the computational advantage of the approach questionable.

The argument underlying the developments in Ref. 12 is that tracking the progression of the crack tip (front) within large elements will restore the sought smooth solution. However, in the numerical results shown, the mesh size still needs to be kept relatively small, even with the enrichment. The reason for this outcome is that tracking the crack tip is not sufficient, but it is also essential to capture the steep gradients in the separation just ahead of the crack tip, slightly under compression. Figure 3 shows the normal opening displacement (u_y) along the interface of a double cantilever beam specimen, obtained from an analysis with ABAQUS generic interface elements, with various mesh sizes as specified: There is no significant discrepancy between the profiles of the normal separation

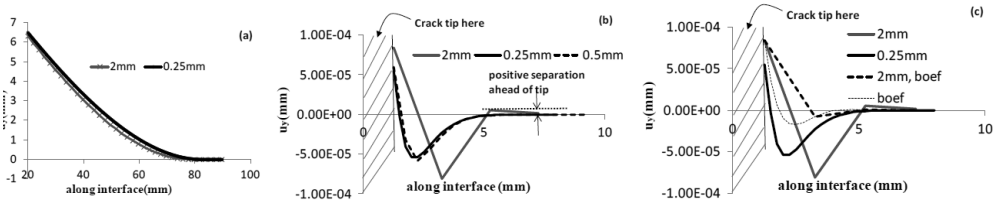


Figure 3. Normal displacement field along the interface of a double cantilever beam. The origin of the axis representing the distance along the interface is the loading point in (a).

https://doi.org/10.1017/S0001924000008617 Published online by Cambridge University Press

along the far field interface, for 2mm and 0·25mm mesh sizes (Fig. 3(a)), but the close-up view of the region just ahead of the tip reveals an entirely different picture (Fig. 3(b)).

For the 2mm mesh, a positive separation can be observed further along the interface and the size of the compressed zone is larger than for the converged meshes. It was also verified with a 5mm mesh that both effects are amplified for larger mesh sizes. Consequences of these observations are:

- premature damage pockets may be numerically created within pristine sections of the interface, causing energy loss without reducing the global load.
- for the crack front to progress, larger values of the crack opening displacement are required in order to bring the large compressed region ahead the crack to the tensile regime.

The approach taken in this work, which was proposed in Guiamatsia *et al*[15], consists of partition-of-unity enrichment, with the analytical solution of a beam on elastic foundation, of the cohesive elements throughout the entire interface, as well as the adjacent solid elements representing the plies. This function is given as per Equation (1) – reference is made to (15) for its derivation – and is plotted in Fig. 3(c) for the 2mm mesh.

$$v = v_0 \varphi(x) = v_0 e^{-\beta x}\left(\mathrm{Cos}\beta x - \mathrm{Sin}\beta x\right),\ \beta = \sqrt[4]{\frac{K}{4EI}} \qquad \ldots (1)$$

In the formula above, x is the distance along the interface from the crack tip, v_0 is the amplitude of the displacement at the crack tip, and β is a constant related to the properties of the beam (Young's modulus E and second moment of area $I = h^3/12$) and of the interface ($K = E_r/t_r$, where E_r is the modulus of the resin and t_r the interface thickness).

This paper uses simple two-dimensional models to study the effects of shape function enrichment under mixed-mode loading conditions. In Section 2, the predicted displacement field along the interface of a double cantilever beam is validated against a converged generic model. Section 3 focuses on the prediction of the response of mixed-mode bending specimens with several methods, including the current enrichment. This is followed by some concluding remarks in Section 4.

2.0 ENRICHED DISPLACEMENT FIELD ALONG A DCB INTERFACE

An implementation of the enriched elements, slightly different to that presented in Ref. 15, was utilised here to study the displacement field along the double cantilever beam considered in Fig. 3. A simple second order topology was considered for the two-dimensional elements (6-node interface and 8-node solid) and the enrichment was implemented through enabling an additional degree of freedom at specific nodes. Here, the 2D interface and solid elements have, respectively, 10 and 14 nodes (Fig. 4), and the enrichment is introduced through the additional nodes. There are two

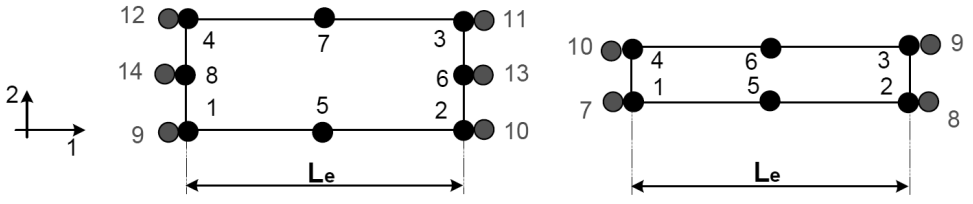


Figure 4. Topology of the 2D enriched elements – left: solid, right: interface.

https://doi.org/10.1017/S0001924000008617 Published online by Cambridge University Press

reasons for this modification: (1) the capability of extra degrees of freedom is not available for the explicit solver of the commercial package used in this work (ABAQUS[19]); (2) the displacement field for all finite elements, including user-defined ones, can be written to the ABAQUS standard output file, while user-defined degrees of freedom are not as readily accessible.

The displacement approximation within the element, in a reference frame where the axes are aligned with the interface element's midplane, is given by:

***Solid*:**

$$u_1(x,y) = N^i(x,y)u_1^i$$

$$u_2(x,y) = N^i(x,y)u_2^i \quad \ldots(2)$$

$$+N^1(x,y)u_1^9\varphi(x)+N^4(x,y)u_1^{12}\varphi(x)+N^8(x,y)u_1^{14}\varphi(x)$$

$$+N^2(x,y)u_1^{10}\psi(x)+N^3(x,y)u_1^{11}\psi(x)+N^6(x,y)u_1^{13}\psi(x) \quad \ldots(3)$$

***Interface*:**

$$u_1(x,y) = N^i(x,y)u_1^i \quad \ldots(4)$$

$$u_2(x,y) = N^i(x,y)u_2^i$$

$$+N^1(x,y)u_1^7\varphi(x)+N^4(x,y)u_1^{10}\varphi(x) \quad \ldots(5)$$

$$+N^2(x,y)u_1^8\psi(x)+N^3(x,y)u_1^9\psi(x)$$

In the above expressions, the index i spans the regular nodes, i.e. $i = 1,8$ for the solid and $i = 1,6$ for the interface; N^i is the (second-order) shape function associated with node i and $\psi(x) = \varphi(L_e\text{-}x)^2$. Henceforth, the enrichment is introduced at the corner nodes on both sides of the elements, for compatibility between adjacent elements and for the convenience of not having to track the position and direction of propagation of the crack tip/front. Hence the normal displacements are $u_2^1 + u_1^7$, $u_2^2 + u_1^8$, $u_2^3 + u_1^9$ and $u_2^4 + u_1^{10}$ for the corner nodes and u_2^5 and u_2^6 for the mid-side nodes. These values were plotted, for the double cantilever beam of Fig. 3 modelled with 5mm enriched elements, and compared to the generic element results using 0·25mm and 2mm meshes in Fig. 5.

As shown, the far-field displacements obtained with the 5mm enriched mesh are more accurate than the 2mm generic element, but more importantly, the representation of the compressed region ahead of the crack tip is closer to the converged solution.

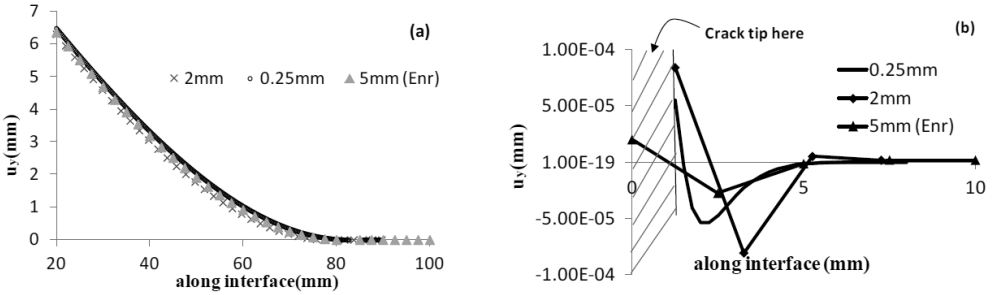


Figure 5. Normal displacement field along the interface of a double cantilever beam. The origin of the axis representing the distance along the interface is the loading point in (a).

https://doi.org/10.1017/S0001924000008617 Published online by Cambridge University Press

This simple exercise shows with a practical example that, along the entire interface including before and ahead of the crack front, the displacement fields obtained with the proposed enriched formulation with a 5mm mesh are very close to the converged field obtained with very small (0·25mm) linear elements. As a result, and this was already shown in Ref. 15, the predicted response in terms of the traction against separation of the beam's arms is in good agreement with the converged response, although there are still oscillations on the softening branch due to the displacement of the crack tip through the elements.

3.0 MIXED-MODE DELAMINATION

As mentioned above, the enrichment is only applied to the normal degree of freedom. Indeed, mode II fracture toughness (G_{IIc}) is usually higher than the mode I fracture toughness (G_{Ic}), and elements of the size targeted here, i.e. 5mm, would usually deliver an acceptable performance for pure mode II loading, as can be seen in Fig. 2. It is therefore legitimate to examine the performance of any strategy addressing the element size issue, with respect to the mode-mixity, considering that practical loading conditions are always a combination of normal and shear failure modes.

For this purpose, the classical benchmarks for quasi-static mixed-mode delamination, tested by Reeder and Crews[17] on AS4/PEEK and reported in Camanho *et al*[16] were studied with two-dimensional models, using a 5mm mesh of enriched elements. The results were compared with the prediction of a converged 0·5mm mesh, as well as 5mm mesh of generic elements in ABAQUS/Explicit. Reference is made to Ref. 16 for the material properties and geometrical details for the specimens. Five different ratios of mode mixity, $k = 0$ (DCB – mode I), 0·2, 0·5, 0·8, 1(ENF – mode II), were considered in the study and the corresponding finite element models with ABAQUS generic elements are shown in Fig. 6. It is noted that in all simulations, except for pure mode I (DCB), a low stiffness layer of solid elements was superposed onto the enriched elements in order to specify the contact between the beam's arms.

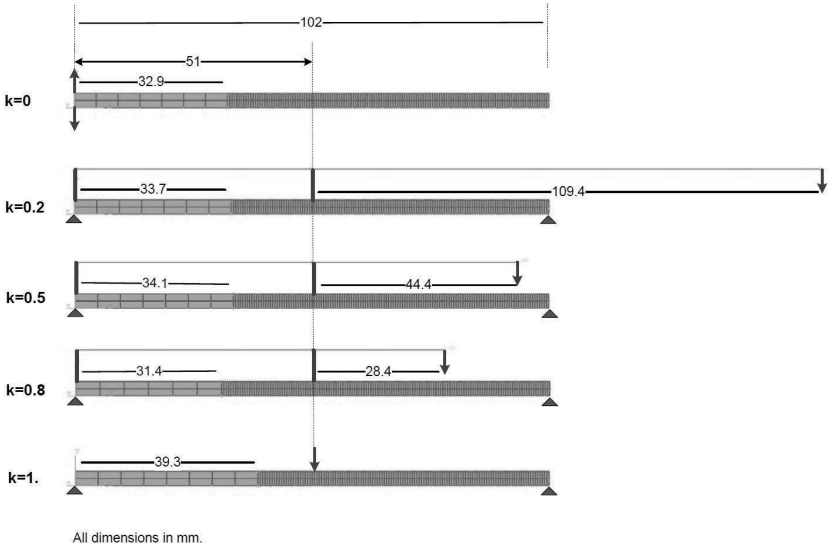


Figure 6. Two-dimensional FE models of the mixed-mode delamination specimens. The load is indicated with arrows and rigid connectors are also shown as straight lines between beam and loading bar. The mesh size of the bonded section is 0·5mm.

https://doi.org/10.1017/S0001924000008617 Published online by Cambridge University Press

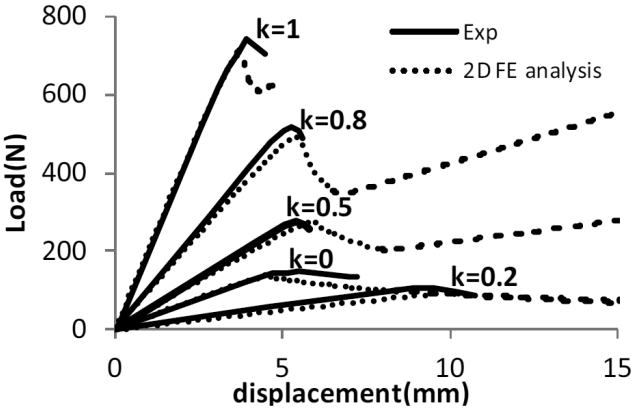


Figure 7. Load against displacement for MMB specimens. The 2D FE models (ABAQUS generic elements) have a 0·5mm mesh size along the bond line. Experimental results as reported in Ref. 16.

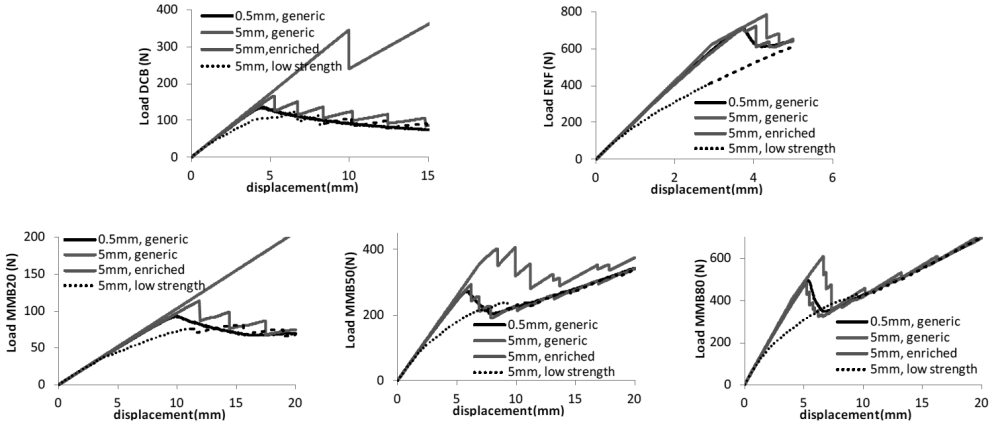


Figure 8. Load against displacement plot for 5mm mesh FE models.

First, the ABAQUS generic model with a 0·5mm mesh is validated against experimental results, for all values of the mode mixity, Fig. 7. Then, for each of the five mode ratios, the prediction of a 5mm mesh model using the current enrichment are contrasted with results produced by Turon *et al*'s low strength approach[8], as well as the converged solution. The corresponding graphs of traction against displacement (or separation) are presented in Fig. 8.

In this study, the artificially low strength considered was one tenth the interface strength, for both shear and normal directions. As reported in other works[10,14], while the approach is successful at accurately tracking the final propagation, it consistently misses the initial peak load in all the cases considered here. In contrast, the enriched element performs significantly better for all the mixed-mode specimens. Although oscillations, resulting from the motion of the crack tip within the large elements, still appear on the global response for cases with dominant mode I damage, the overall prediction is very good. Moreover, the curves relating the minimum peaks of the traction against separation plot could be used as a design strategy as suggested in Davies and Guiamatsia[18].

https://doi.org/10.1017/S0001924000008617 Published online by Cambridge University Press

These results show that the performance of the enrichment improves as the mode mixity varies from 0 to 1, which is somehow expected given the increasing size of the fracture process zone when the partition of mode II dissipation increases.

3.1 Computational cost

The total clock time required for the analysis of each of the mixed-mode specimens is reported in Table 1.

Table 1
Clock time (in seconds) reported in ABAQUS .msg file

Specimen	0·5mm generic	5mm low strength	5mm enriched
DCB	420	69	227
MMB 20	420	87	183
MMB 50	340	99	221
MMB 80	128	83	286
ENF	121	57	182

As expected, the low strength approach yields the best computational benefits, however with the poor results shown earlier. Although larger computing times are recorded for the MMB 80 and ENF specimens, the computing times for the enriched model is generally lower than that of the converged 0·5mm generic model.

The real computational savings generated by the enrichment are, however, more significant than conveyed by Table 1, for at least two reasons:

- The enriched elements (solid and interface) are user-defined elements, external components that are not optimised for ABAQUS' solvers. For the Explicit solver in particular, specific code organisation is required in order to optimise the performance and this is being undertaken at the moment.
- In order to specify contact between the beam arms (in all cases but the DCB), an additional layer of low stiffness ABAQUS generic elements are superposed on the enriched ones for the surface definition. This results in a larger assembled matrix being sent to the implicit solver, hence a larger solution time. This would be avoided if it was possible to define contact between two-node based surfaces, for example.

4.0 CONCLUDING REMARKS

This paper presented a study on the performance of enriching second-order interface and solid elements, with the analytical solution of a beam on elastic foundation, for the study of mixed-mode delamination. The formulation was implemented with a 10-node interface element and a 14-node solid element, using extra nodes to provide the additional degrees of freedom needed for the enrichment. It was shown that the enriched elements performed consistently well, throughout the entire spectrum of mixed-mode ratios considered, with elements as large as 5mm yielding results with a very high level of accuracy, and more than suitable for industrial design purposes.

https://doi.org/10.1017/S0001924000008617 Published online by Cambridge University Press

REFERENCES

1. SCHELLEKENS, J.C.J. and DE BORST, R. A non-linear finite element approach for the analysis of mode I free edge delamination in composites, *Int J Solids and Structures*, 1993, **30**, pp 1239-1253.
2. DUGDALE, D.S. Yielding of steel sheets containing slits, *J Mechanics and Physics of Solids*, 1960, **8**, pp 100-104.
3. BARENBLATT, G.I. The mathematical theory of equilibrium cracks in brittle fracture, *Advances in Applied Mechanics*, 1962, **7**, pp 55-129.
4. XIE, D. and WAAS, A.M. Discrete cohesive zone model for mixed-mode fracture using finite element analysis, *Engineering Fracture Mechanics*, 2006, **73**, pp 1783-1796.
5. ALLIX, O. and CORIGLIANO, A. Modeling and simulation of crack propagation in mixed-modes interlaminar fracture specimens, *Int J Fracture*, 1996, **77**, pp 111-140.
6. DAVIES, G.A.O., HITCHINGS, D. and ANKERSEN, J.K. Predicting delamination and debonding in modern aerospace composite structures, *Composites Science and Technology*, 2006, **66**, pp 846-854.
7. GUSTAFSON, P.A. and WAAS, A.M. Efficient and robust traction laws for the modelling of adhesively bonded joints. in 49th AIAA SDM Conference. Schaumburg, IL, USA, 7-10 April 2008.
8. TURON, A., CAMANHO, P.P., COSTA. J. and DAVILA, C.G. An engineering solution for mesh size effects in the simulation of delamination using cohesive zone models, *Engineering Fracture Mechanics*, 2007, **74**, pp 1665-1682.
9. CRISFIELD, M.A. and ALFANO, G. Adaptive hierarchical enrichment for delamination fracture using a decohesive zone model, *Int J for Numerical Methods in Engineering,* 2002, **54**, pp 1369-1390.
10. HARPER, P.W. and HALLETT, S.R. Cohesive zone length in numerical simulations of composite delamination, *Engineering Fracture Mechanics*, 2008, **75**, pp 4774-4792.
11. SAMIMI, M., VAN DOMMELEN, J.A.W. and GEERS, M.G.D. An enriched cohesive zone model for delamination in brittle interfaces, *Int J Numerical Methods in Engineering*, 2009, **80**, pp 609–630.
12. SAMIMI, M., VAN DOMMELEN, J.A.W. and GEERS, M.G.D. A self-adaptive finite element approach for simulation of mixed-mode delamination using cohesive zone models, *Engineering Fracture Mechanics*, 2011, **78**, pp 2202–2219.
13. VAN DER MEER, F.P., MOES, N. and SLUYS, L.J. A level set model for delamination – modelling crack growth without cohesive zone or stress singularity. Engineering Fracture Mechanics, 2012, **79**, pp 191-212.
14. VAN DER MEER, F.P., SLUYS L.J., HALLETT, S.R. and WISNOM, M.R. Computational modelling of complex failure mechanisms in laminates, *J Composite Materials*, 2012, **43**, pp 603-623.
15. GUIAMATSIA, I., ANKERSEN, J.K., DAVIES, G.A.O. and IANNUCCI, L. Decohesion finite element with enriched basis functions for delamination, *Composites Science and Technology*, 2009, **69**, pp 2616-2624.
16. CAMANHO, P.P., DAVILA, C.G. and DE MOURA, M.F. Numerical simulation of mixed-mode progressive delamination in composite materials. *J Composite Materials*, 2003, **37**, pp 1415-1438.
17. REEDER, J.R. and CREWS, J.H. Mixed-mode bending method for delamination testing, *AIAA J*, 1990, **28**, pp 1270-1276.
18. DAVIES, G.A.O. and GUIAMATSIA, I. The problem of the cohesive zone in numerically simulating delamination/debonding failure modes, *Applied Composite Materials*, 2012, **19**, pp 837-838.
19. ABAQUS, Simulia Inc. Theory manual, version 6.9. Edition 2010.

https://doi.org/10.1017/S0001924000008617 Published online by Cambridge University Press